Planta (1994) 193:67–73

Planta

Regulation of electrical coupling between *Arabidopsis* root hairs

Roger R. Lew

Biology Department, York University, 4700 Keele Street, North York, Canada M3J 1P3;
FAX: 1 (416) 736 5698; Tel.: 1 (416) 736 2100 ext. 66114

Received: 26 July 1993 / Accepted: 14 September 1993

Abstract. Voltage clamp was used to measure the voltage dependence of cell-to-cell coupling via plasmodesmata between higher-plant cells (root hairs of *Arabidopsis thaliana* (L.) Heynh.). In addition, ionophoresis was used to introduce a variety of ions [Ca^{2+}, inositol-trisphosphate, Li^+, K^+, Mg^{2+}, ethylene glycol-bis(β-aminoethyl ether)-N,N,N′,N′-tetraacetic acid (EGTA), 1,2-bis(2-aminophenoxy)ethane-N,N,N′,N′-tetraacetic acid (BAPTA), H^+, and OH^-] to examine whether they regulate cell-to-cell coupling. Electrical coupling showed high variability in this single cell type at the same developmental stage; the coupling ratio ranged from near 0% to about 90% with a mean value of 32%. It was voltage independent for intracellular voltage gradients (transplasmodesmatal) of −163 to 212 mV. While Ca^{2+} closes the plasmodesmatal connections (at concentrations higher than those causing cessation of cytoplasmic streaming), inositol-trisphosphate and lithium are without effect. Apparently, inositol-trisphosphate may not cause increased cytosolic Ca^{2+} in root hairs. Alkalinization by OH^- ionophoresis caused a modest decline in cell-to-cell coupling, as did acidification by H^+ ionophoresis (to an extent causing the cell to become flacid). Increases in cytosolic K^+, Mg^{2+}, and the calcium chelator BAPTA by ionophoresis had no effect on cell-to-cell coupling. The regulation (and lack thereof) reported here for plant plasmodesmata is quite similar to that of gap junctions.

Key words: *Arabidopsis* (root hairs) – Calcium – Electrical coupling of cells (pH, voltage) – Inositol trisphosphate – Plasmodesma

Introduction

Plasmodesmatal connections are the basis for a symplasmic pathway between plant cells (Robards and Lucas 1990). They are the functional equivalent of gap junctions in animal cells as a means for intracellular communication. The discovery of a gap-protein homologue in *Arabidopsis* (Meiners et al. 1991) suggests that the functional equivalence may be closer than previously suspected. To address this, there is a clear need for detailed characterization of the regulation of plasmodesmatal connections (Reid and Overall 1992) for comparisons with gap junctions (Beyer 1993).

Ordinarily, plasmodesmata exclude molecules of molecular weight greater than about 800 (Tucker 1982; Goodwin 1983; Terry and Robards 1987), as measured by conjugated dye movement between cells. There are reports that cell-to-cell coupling is regulated: a) by pressure gradients (Coté et al. 1987; Ding and Tazawa 1989; Reid and Overall 1992) in *Chara*; b) by plasmolysis (Drake et al. 1978; Erwin and Goodwin 1984); c) by phytochrome (Racusen 1976); d) by calcium (Baron-Epel et al. 1988; Tucker 1990) (although Reid and Overall [1992] found calcium had no effect on coupling); and e) by inositol-trisphosphate (Tucker 1988). In animal cells, increased Ca^{2+}, intracellular voltage gradients, and pH are known to regulate cell-to-cell coupling (Spray 1990). These factors are examined in this study using *Arabidopsis* root hairs.

The methodology of electrical coupling (Turin 1984) in its simplest form of direct current injection has been previously used in *Chara* (Coté et al. 1987; Ding and Tazawa 1989; Reid and Overall 1992), *Elodea* (Spanswick 1972), oat coleoptile cells (Racusen 1976; Drake et al. 1978), *Trianea bogotensis* roots (Vorob'ev et al. 1982), and *Azolla* roots (Overall and Gunning 1982). In this study, voltage clamping makes it possible to measure the voltage dependence of cell-to-cell coupling reported in some gap junctions (Spray 1990; Beyer 1993). Ionophoresis was used to introduce a variety of ions: Ca^{2+}, inositol-trisphosphate, Li^+, K^+, Mg^{2+}, EGTA, BAPTA, H^+ and OH^- into one of the two cells used for measurements of cell-to-cell coupling to determine their effect on coupling.

Abbreviations: BAPTA = 1,2-bis(2-aminophenoxy)ethane-N,N,N′,N′-tetraacetic acid

Materials and methods

Seeds of *Arabidopsis thaliana* (L.) Heynh. (*Columbia* wild type) were sown on 0.9% gellan gum in artificial pond water (APW) 5 [0.1 mM KCl, $CaCl_2$, and $MgCl_2$; 1.0 mM 2-(N-morpholino)ethanesulfonic acid (Mes); and 0.2 mM Na_2SO_4; pH adjusted to 5.0 with NaOH] as previously reported (Lew 1991). After one to two weeks, APW 7 [0.1 mM KCl, $CaCl_2$, and $MgCl_2$; 1.0 mM 3-(N-morpholino)propanesulfonic acid (Mops); and 0.5 mM NaCl; pH adjusted to 7.0 with NaOH] was added to the culture dishes. Within a few hours, pairs of epidermal cells end-to-end on a longitudinal cell row with root-hair extensions were chosen and impaled when the root-hair extensions of the younger of the two cells had reached a length of 40–80 μm. Typically, cells with actively growing root hairs were used.

The micropipette used to impale the older of the two root hairs was double-barreled (Lew 1991) for voltage-clamp measurements. Voltage-clamping protocols have been described previously (Lew 1991). Briefly, an operational amplifier configured for voltage-clamping was used in conjunction with a data-acquisition board (Scientific Solutions, Cleveland, Ohio, USA) via compiled C programs that controlled the voltage clamp and monitored the clamped voltage and clamping current, and, in these double cell impalements, the voltage of the second cell. The voltage-clamping protocol was a bipolar staircase of clamped voltages of 50 ms duration. The younger of the two adjacent hairs was impaled with a single-barreled micropipette containing a variety of ions which were ionophoresed into the cell with currents no higher than ±10 nA.

Three methods were used to measure the extent of electrical coupling between the adjacent, end-to-end cells on the longitudinal cell row.

Method one. A 1-nA current was passed through one barrel of the double-barreled micropipette. The other barrel measured the voltage deflection in the older root hair, while the voltage deflection in the younger root hair was measured with the single-barreled micropipette. The ratio of the two voltage deflections (× 100) yields the coupling ratio as a percentage.

Method two. Voltage-clamp measurements in the older root hair result in voltage changes in the younger root hair due to current leakage through the plasmodesmata. The voltages in both cells, and the current injection were measured via a data-acquisition system and used to examine the voltage dependence (that is, the effect of the electrical gradient between the cells) of cell-to-cell coupling.

Method three. Ionophoretic currents (electrically injecting ions) in the single-barreled micropipette caused a voltage deflection in the older, adjacent root hair. Changes in the extent of that deflection as ionophoresis continued yields a measurement of the percentage change in coupling between the two cells. This was used to assess the regulation of coupling by the ionophoresed ion.

Results and discussion

Measurements of cell-to-cell coupling. An example of a typical experiment is shown in Fig. 1 for ionophoresis of Mg^{2+} from a micropipette containing 50 mM $MgCl_2$ and 100 mM KCl. Using the ionic conductances at infinite dilution (Castellan 1971, p. 724) (Mg^{2+}, 53.0 (S/cm) (equiv/cm^3); K^+ 73.5; Cl 76.4) and concentrations, the expected contribution of Mg^{2+} to the total current is 10.5%. For a 500-nanocoulomb (nC) injection into the cell (about 14 pl volume), this results in an estimated concentration of 40 mM in the cell. This estimate is an upper limit since sequestration and leakage into adjacent cells will also occur.

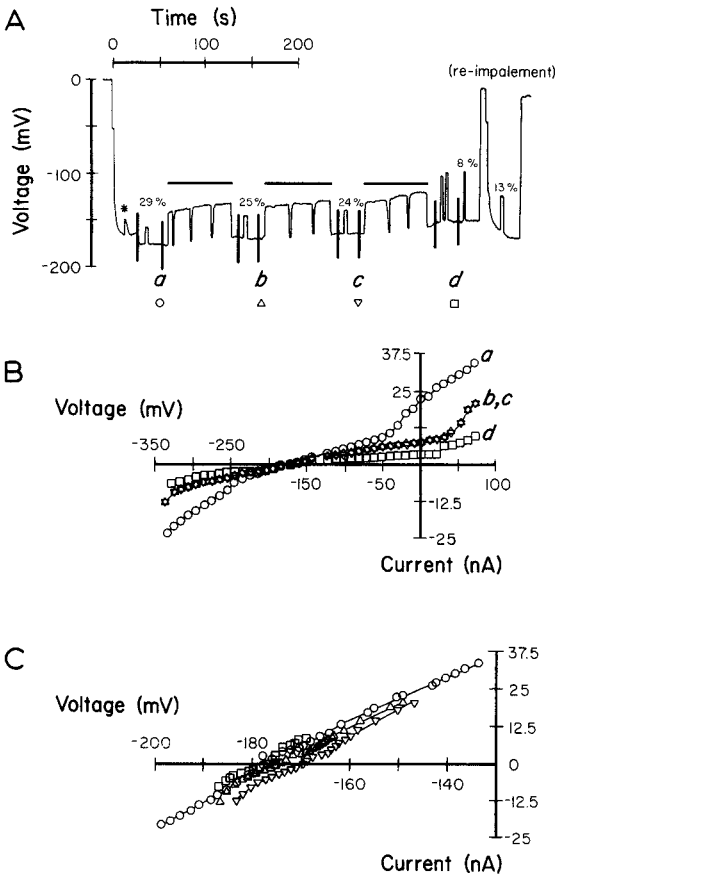

Fig. 1A–C. Electrical cell-to-cell coupling experiments between *Arabidopsis* root hairs and the effect of Mg^{2+} ionophoresis. The experiment shown is an example of the three methods used to measure electrical coupling between *Arabidopsis* root hairs as outlined in the *Materials and methods* section. The membrane potential for the older, impaled cell is shown in **A**. About 15 s after impalement, the younger cell was impaled. This caused a transient depolarization in the older cell marked by an *asterisk*. A 1-nA current pulse was injected into the first, older cell at various times and is marked by the calculated coupling ratio (as a percentage; voltage deflection in cell two divided by the deflection in cell one multiplied by 100) (Method one). Current-voltage measurements in the first, older cell are marked by vertical bars; four are shown in **B** as marked (*a,b,c*, and *d*). The clamping current versus the voltage in the second, younger cell is shown in **C** for the same current-voltage measurements (Method two). The *horizontal bars* just above the membrane-potential trace in **A** mark the periods during which a +5-nA current was injected into the second, younger cell, resulting in a depolarized voltage deflections in the first, older cell as shown. The current was turned off occasionally to monitor changes in the extent of the voltage deflection (Method three). Note that Mg^{2+} ionophoresis caused a decline in conductance for the current-voltage relations (compare *a,b*, and *c* in **B**) even though the coupling ratio did not change. After about 350 s, the coupling ratio did decline, but recovered to a higher level upon re-impalement of the first, older cell (as marked). This indicates that coupling ratios measured after prolonged impalements may be inaccurate due to plugging of the double-barreled micropipette

First, the older root hair was impaled with the double-barreled micropipette. About 15 s later, the younger root hair was impaled with the single-barreled micropipette, causing a transient depolarization of about 20 mV in the older cell (Fig. 1A). Current-voltage measurements were

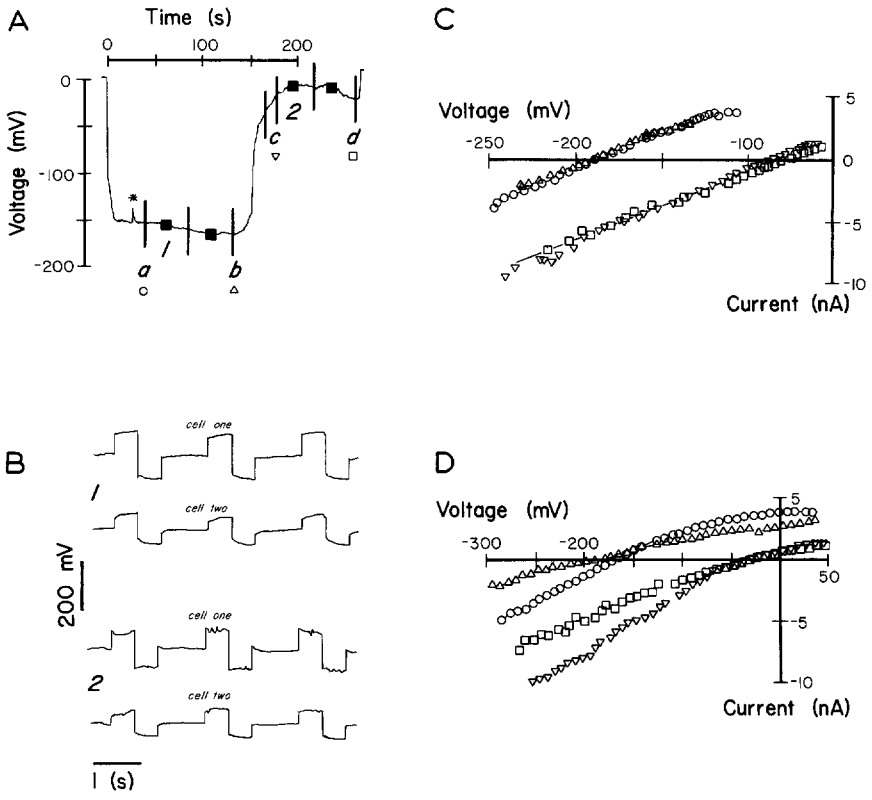

Fig. 2A–D. Clamping current experiments between *Arabidopsis* root hairs. Long-term modulation of the voltage difference between adjacent root hairs required direct current pulses rather than voltage clamping due to clipping of the clamping currents. **A** As described in Fig. 1. Current pulses were passed through one barrel of the double-barreled micropipette and the voltage deflections in the first and second cell monitored as shown in **B** before (1) and after (2) treatment with 5–10 mM vanadate. Capacitative coupling spikes at the onset of the current pulses are not shown. Clamping current versus voltage deflection in the second, younger cell is shown in **C**, and current-voltage relations for the first, older, cell are shown in **D** for the times marked (*a,b,c*, and *d*). Vanadate (5–10 mM) was added a few seconds after the current-voltage measurement *b* in **A** and caused a marked depolarization. Note that there is no significant change in voltage deflections due to current-pulsing in **B**, indicating that voltage dependence does not occur after periods of time as long as 0.5 s, also indicated by the linearity of the current versus voltage deflections in the second, younger cell in **C** for the 50-ms voltage-clamping treatment. Furthermore, the plasma-membrane H^+-pump inhibitor, vanadate, does not affect cell-to-cell coupling

performed, then a 1-nA current was injected into the older cell. This caused a 17-mV depolarization in the older cell and a 5-mV depolarization in the younger cell, resulting in a calculated coupling of 29%. A subsequent 5-nA ionophoresis into the younger root hair caused a 37-mV depolarization in the older cell. The ionophoretic current was occasionally turned off to allow measurements of the voltage deflection in the older cell at various times. After about 70 s of ionophoresis, current-voltage relations and electrical coupling were re-measured. The whole process was repeated three times. After the third ionophoretic treatment, the coupling ratio had declined to 8%. This decline was due to plugging of the double-barreled micropipette which was not completely cleared (coupling returned to 13%) after removal and re-impalement with the double-barreled micropipette. Thus, long-term measurements of electrical coupling (as percentage coupling) may be problematic. However, the voltage deflection caused by ionophoresis remained constant, and this was used to assess the effect of ionophoresis on the extent of coupling.

Current-voltage relations for the older cell are shown in Fig. 1B. Ionophoresis into the younger cell caused a decrease in the conductance of the current-voltage relation of the older adjacent cell without affecting the extent of electrical coupling. This implies that Mg^{2+} was able to diffuse through the plasmodesmata into the adjacent cell, affecting its current-voltage relations. The decreased conductance observed with Mg^{2+} ionophoresis was not observed with any of the other ions used in this study.

Trans-plasmodesmatal voltage gradients. A comparison of the current injected into the older cell and the voltages in both the older and younger cells allows us to determine whether the voltage gradient between the two cells regulates the extent of coupling (Fig. 1B, C). The linearity of the current-voltage relation for the younger cell (Fig. 1C) indicates that electrical coupling is unaffected by voltage gradients of -140 mV to 210 mV (treating the younger cell as reference ground) between the two cells. For experimental runs with K^+ or Mg^{2+} ionophoresis, using experiments where voltage deflections were large (such as in Fig. 1C), the range of voltage differences between the adjacent cells was -163 mV to 212 mV, with mean ($\pm$ SD) values of -91 ± 56 to 125 ± 45 mV ($n = 7$). In all cases, the current-voltage relations were linear, indicating no voltage dependence of electrical coupling.

For gap junctions, transjunctional voltage dependence of gap-junction conductance varies with species and tissue type, and is common in embryonic tissue (Spray 1990). When it does occur, it is readily seen in the voltage range of -100 to 100 mV. For *Arabidopsis* root hairs, it is not apparent with a voltage clamp of 50 ms duration over a wider voltage range. Unfortunately, voltage-dependent clamping currents increase to clipping levels if a longer voltage-clamp duration is used. Therefore, to assess the effect of a longer-duration voltage difference between the two cells, constant current pulses through one barrel of the double-barreled micropipette were used while voltage was monitored in both cells. An example experiment is shown in Fig. 2. During 0.5-s cur-

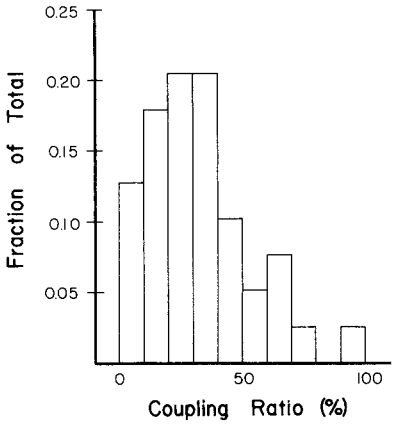

Fig. 3. The distribution of coupling ratios (as a percentage). Initial measurements of the coupling ratio were compiled and are shown as a frequency histogram. Most measurements clustered at values between 10 and 30%, with a significant number of lower and higher values. The mean value and other statistics are presented in the *Results and discussion* section

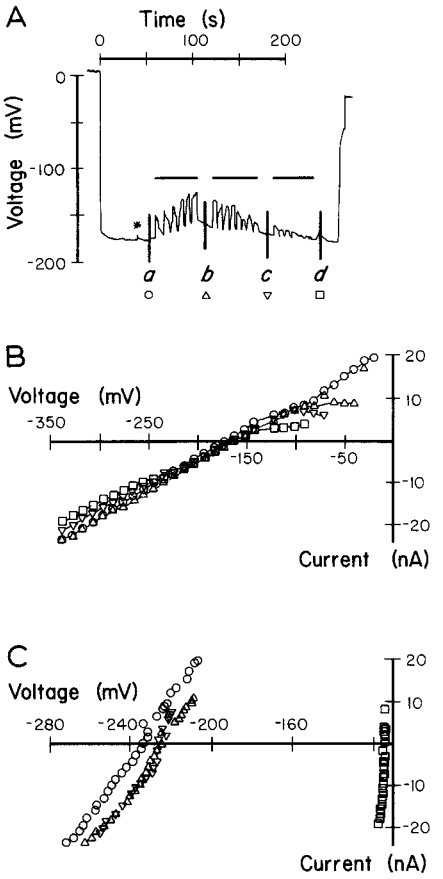

Fig. 4A–C. Effect of calcium ionophoresis on the extent of coupling. As in Figs. 1A and 2A, **A** shows the impalement of the first, older cell. The *horizontal bars* above the trace in **A** mark the period during which a +5-nA current was injected into the second, younger cell, causing a depolarization in the first, older cell due to cell-to-cell coupling. The ionophoretic current was turned off at intervals of about 10 s. Current-voltage measurements in the first, older cell were made at the *vertical bars* and are shown in **B** as marked (*a,b,c*, and *d*), while clamping currents versus voltage deflections in the second, younger cell are shown in **C**. Coupling ratios were not performed in the experiment. Note the decline in voltage deflections during Ca^{2+} ionophoresis which returned to near initial levels when the ionophoretic current was turned off and then on again. This is probably due to plugging of the single-barreled micropipette tip due to high Ca^{2+} at the tip during ionophoresis, which disappears as Ca^{2+} diffuses away from the tip when the ionophoretic current is turned off. This was often, though not always, observed. The decline in electrical coupling observed in **A** as smaller and smaller voltage deflections is confirmed by measurements of the clamping current versus voltage deflection which shift to a vertical slope as shown in **C**. In experiments in which the coupling ratio was measured, the coupling ratio also approached zero

rent injections into the older cell, there was no change in the voltage deflection in the younger cell, indicating there was no time-dependent component of voltage dependence. A similar result has been reported for *Chara* (Reid and Overall 1992) for even longer current injections, and in *Trianea bogotensis* (Vorob'ev et al. 1982), but for much lower voltage deflections (–24 to 40 mV). In the experiment shown in Fig. 2, the effect of vanadate (an inhibitor of the plasma-membrane H^+ pump) on coupling was examined. Inhibition of the pump, resulting in a large depolarization of the membrane potential (111 ± 31 mV, $n = 5$), did not affect the electrical coupling ratio (before: 34%; after: 36%).

Coupling ratios. The distribution of electrical-coupling ratios, using only the initial measurements to avoid the problem of plugging of the double-barreled micropipette as the experiment progressed, is shown in Fig. 3. The mean ($\pm$SD) was 32% ± 21 ($n = 39$); the median was 29%. There was a broad range of values from near zero to 95%. Broad intra-species values (from 9 to 79%) have been reported (Robards and Lucas 1990). In this study, electrical coupling shows high population variance in a single cell type at a fairly specific developmental stage at a seedling age of one to two weeks. It is unlikely that this wide range is due to insertion into the vacuole (cf. Vorob'ev et al. 1982); the microelectrode tip is commonly located in the cytoplasm, based upon the initial distribution of dyes injected into the root hair. Wounding effects on cell-to-cell coupling may also be discounted since cytoplasmic streaming can be observed after the impalement and the cells continue to grow (Lew 1991).

Calcium regulates cell-to-cell coupling. An example of Ca^{2+} ionophoresis is shown in Fig. 4. The ionophoretic micropipette contained 50 mM $CaCl_2$ and 100 mM KCl. The ionic conductance of Ca^{2+} is 59.5 (S/cm) (equiv/cm^3), so the expected contribution of Ca^{2+} to total current is about 13.2%. This gives an upper limit of increasing Ca^{2+} concentration to about 40 mM with a 500-nC injection, bearing in mind that sequestration must also be occurring (the estimated cytosolic Ca^{2+} increase is 10–70 μM, see below). When cytoplasmic streaming could be observed, it stopped within seconds of the onset of ionophoresis. Considerably longer periods of ionophoresis were required to block almost completely the plasmodesmatal pores. The current-voltage relations for the older cell were unaffected, but the membrane potential of

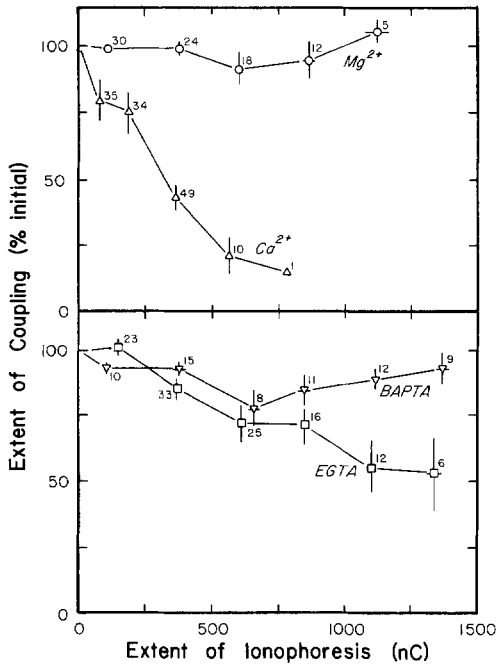

Fig. 5. Effect of Ca^{2+}, Mg^{2+}, and Ca^{2+} chelators on the extent of cell-to-cell coupling. The extent of ionophoresis is presented as nanocoulombs of charge injected into the cell. For Mg^{2+} (○—○) and Ca^{2+} (△—△), the amount of ion injection as concentration change in the cell is calculated in the *Results and discussion* section. For the chelators (*lower panel*), ionic conductivity values are not known and would vary with pH. Horizontal and vertical bars (when not hidden by the symbols) represent standard errors. Sample sizes are marked by each symbol. Note that the chelator EGTA (□—□) does cause a decline in cell-to-cell coupling, but this is probably not due to Ca^{2+} chelation since BAPTA (▽—▽) is without effect

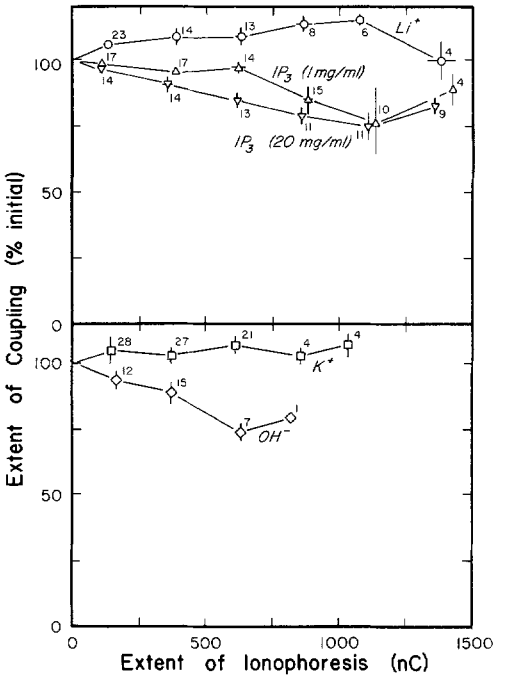

Fig. 6. Effect of Li^+, inositol-trisphosphate, K^+ and OH^- on the extent of cell-to-cell coupling. The extent of ionophoresis is presented as nanocoulombs of charge injected into the cell. Li^+ (○—○) and inositol-trisphosphate (△—△: 1 mg/ml in 20 mM KCl; ▽—▽: 20 mg/ml in dH_2O) had no significant effect. Cytoplasmic streaming was observed to continue during inositol-trisphosphate ionophoresis. Potassium (□—□) and OH^- (◇—◇) are shown in the *lower panel*. Horizontal and vertical bars (when not hidden by the symbols represent standard errors. Sample sizes are marked by each symbol

the younger cell was depolarized, and the slope of the current-voltage relation for the younger cell shifted to a vertical position as electrical coupling declined. It is likely that little Ca^{2+} moved through the plasmodesmatal connections into the older cell, since its membrane potential was unaffected by Ca^{2+} ionophoresis.

For Ca^{2+} ionophoresis (and Mg^{2+}, and two Ca^{2+} chelators, EGTA, BAPTA), the extent of ionophoresis as nanocoulombs of charge passed into the cell was compared to the changes in the extent of electrical coupling (as a percentage of the initial) and is shown in Fig. 5. Magnesium was used as a control divalent cation. It does not affect the extent of coupling. As little as 400 nC of Ca^{2+} ionophoresis cause a decline in coupling below 50% of the initial value. But this is high compared to the amount of ionophoresis required to inhibit cytoplasmic streaming (about 70 nC). It is known that cytoplasmic streaming is inhibited at 1–10 μM Ca^{2+} (Williamson 1992). Assuming Ca^{2+} increases are a linear function of the extent of ionophoresis, this means that coupling is inhibited 50% at 10–70 μM cytosolic Ca^{2+}. This is analogous to the situation with gap junctions, where Ca^{2+} is known to close the junctions, but at levels that are too high to be considered physiologically relevent unless severe wounding has occurred (Spray 1990).

To assess whether a decrease in cytosolic Ca^{2+} concentrations affects coupling, the Ca^{2+} chelators EGTA (100 mM, pH 7 with KOH) and BAPTA (100 mM, tetrapotassium salt) were used. While EGTA did cause a decline to almost 50% of initial coupling with about a 1400-nC injection, BAPTA was without effect. Even with about 2100 nC of BAPTA injection, coupling was still about 90% of the initial coupling ($n = 5$; data not shown). It appears that EGTA has additonal deleterious effects compared to BAPTA. The conductivity of these two chelators is not known, but if one assumes that about 5% of the current will be carried by the chelator, then the internal concentration will be in the range calculated for Mg^{2+} and Ca^{2+} (about 40 mM). Apparently, decreases in cytosolic Ca^{2+} do not affect electrical coupling.

Inositol-trisphosphate. Given the dependence of electrical coupling on Ca^{2+}, the effect of *myo*-inositol 1,4,5-trisphosphate was also examined. Inositol-trisphosphate is known to cause an increase in cytoplasmic Ca^{2+} by inducing its release from internal stores (Berridge 1984). Either 1 mg/ml in 20 mM KCl, or 20 mg/ml in dH_2O was used. The effect on coupling was minimal (Fig. 6). Tucker (1988) reported that inositol-trisphosphate did inhibit coupling in *Setcreasea* staminal hairs. No effect was ob-

served in *Arabidopsis* root hairs even with higher concentrations than Tucker (1988) used (20 mg/ml compared to 10 mg/ml) as well as ionophoresis (Tucker [1988] used simple diffusion from the micropipette tip). Lithium (100 mM LiCl; a 500-nC injection would result in cytosolic [Li^+] increasing to an upper limit of 75 mM), an inhibitor of the inositol-trisphosphate pathway (it inhibits *myo* inositol-1-phosphatase causing a decline in phosphoinositides; Berridge 1984) was also without effect. Furthermore, even after extended ionophoresis, cytoplasmic streaming could be observed, unlike reported observations in *Setcreasea* and *Acetabularia* (Allen and O'Connor 1990). It is possible that, although there is evidence for the inositol-trisphosphate pathway in higher plants (cf. Coté and Crain 1993), it is absent in *Arabidopsis* root hairs using ionophoretic techniques and monitoring cytoplasmic streaming and cell-to-cell coupling. Alternatively, inositol-trisphosphate may induce an increase in Ca^{2+} insufficient to inhibit cytoplasmic streaming.

Potassium and cell pH. The effect of K^+ (as a monovalent cation control), H^+ and OH^- were also examined. While K^+ had no effect upon the extent of coupling, OH ionophoresis caused a slight decline to about 75% of initial coupling with about 500 nC of injection (Fig. 6). Injections of up to 121 nC of H^+ were without effect (coupling was 100% of initial). In two experiments with H^+ ionophoresis, coupling did decline, but the cells were flaccid, suggesting that an effect of acidification-induced cellular damage on coupling was being observed. The amount released into the cell can be calculated based upon ionic conductivities (Castellan 1971) (H^+, 349.8 (S/cm) (equiv/cm^3); Cl^-, 76.35; OH^-, 197.8; Na^+, 50.11) and concentrations: the expected contribution of OH^- would result in an increase in [OH^-] of about 300 mM for a 500-nC injection, and, an increase in [H^+] of about 61 mM for a 100-nC injection. These are upper limits which would be decreased by sequestration, efflux, and cytoplasmic pH buffering. It appears that cell-to-cell coupling is inhibited by either alkalinization or acidification; the extent of the actual change in cytosolic pH is not known, but probably high given that H^+ ionophoresis sufficient to affect coupling also damaged the cell.

Summary

Voltage clamping and ionophoresis have made it possible to characterize regulatory aspects of cell-to-cell coupling via plasmodesmata in higher-plant cells, between *Arabidopsis* root hairs. The electrical coupling is voltage independent and inhibited by high, non-physiological, Ca^{2+} concentrations. Inhibition by high H^+ concentrations appears to be due to obvious cellular damage; OH^- injection also decreased cell-to-cell coupling. The monovalent, K^+, and the divalent, Mg^{2+} (which appears to pass through the plasmodesmata) were without significant effects, as was the Ca^{2+} chelator BAPTA. Interestingly, the inositol-trisphosphate pathway may not function in this cell type.

In general, it appears that higher-plant plasmodesmata do exhibit similar regulatory properties to those of gap junctions. In particular, transjunctional voltage independence is often seen for gap junctions (Spray 1990), as is inhibition of coupling by elevated Ca^{2+} concentrations and acidification. With single-cell voltage clamps, current noise (about 40 pA) is too high to resolve single channels, but hopefully voltage clamping of both cells may uncover the molecular channel events of plasmodesmata, analogous to those observed with gap junctions (Spray 1990).

References

Allen, N.S., O'Connor, S.A. (1990) Inhibition of intracellular particle motions in *Acetabularia acetabulum* L. by phosphoinositides. In: Inositol metabolism in plants, pp. 301–310. Morré, D.J., Boss, W.F., Loewus, F.A., eds. Wiley-Liss, New York

Baron-Epel, O., Hernandez, D., Jiang, L.-W., Meiners, S., Schindler, S. (1988) Dynamic continuity of cytoplasmic and membrane compartments between plant cells. J. Cell Biol. **106**, 715–721

Berridge, M.J. (1984) Inositol trisphosphate and diacylglycerol as second messengers. Biochem. J. **220**, 345–360

Beyer, E.C. (1993) Gap junctions. Int. Rev. Cytol. **137C**, 1–37

Castellan, G.W. (1971) Physical chemistry. 2nd ed. Addison-Wesley. Reading, Massachusetts

Coté, G.G., Crain, R.C. (1993) Biochemistry of phosphoinositides. Annu. Rev. Plant Physiol. Plant Mol. Biol. **44**, 369–419

Coté, R., Thain, J.F., Fensom, D.S. (1987) Increase in electrical resistance of plasmodesmata of *Chara* induced by an applied pressure gradient across the node. Can. J. Bot. **65**, 509–511

Ding, D.-Q., Tazawa, M. (1989) Influence of cytoplasmic streaming and turgor pressure gradient on the transnodal transport of rubidium and electrical conductance of *Chara corallina*. Plant Cell Physiol. **30**, 739–748

Drake, G.A., Carr, D.K., Anderson, W.P. (1978) Plasmolysis, plasmodesmata, and the electrical coupling of oat coleoptile cells. J. Exp. Bot. **29**, 1205–1214

Erwin, M.G., Goodwin, P.B. (1984) Characterization of the *Egeria densa* Planch. leaf symplast: response to plasmolysis, deplasmolysis, and to aromatic amino acids. Protoplasma **122**, 162–168

Goodwin, P.B. (1983) Molecular size limit for movement in the symplast of *Elodea* leaf. Planta **157**, 124–130

Lew, R.R. (1991) Electrogenic transport properties of growing *Arabidopsis* root hairs. The plasma membrane proton pump and potassium channels. Plant Physiol. **97**, 1527–1534

Meiners, S., Xu, A., Schindler, M. (1991) Gap junction protein homologue from *Arabidopsis thaliana*: evidence for connexins in plants. Proc. Natl. Acad. Sci. **88**, 4119–4122

Overall, R.L., Gunning, B.E.S. (1982) Intercellular communication in *Azolla* roots: II Electrical coupling. Protoplasma **111**, 151–160

Racusen, R.H. (1976) Phytochrome control of electrical potentials and intercellular coupling in oat-coleoptile tissue. Planta **102**, 215–227

Reid, R.J., Overall, R.L. (1992) Intercellular communication in *Chara*: factors affecting transnodal electrical resistance and solute fluxes. Plant Cell Environ. **15**, 507–517

Robards, A.W., Lucas, W.J. (1990) Plasmodesmata. Annu. Rev. Plant Physiol. Plant Mol. Biol. **41**, 369–419

Spanswick, R.M. (1972) Electrical coupling between cells of higher plants: A direct demonstration of intercellular communication. Planta **102**, 215–227

Spray, D.C. (1990) Electrophysiological properties of gap junction channels. NATO ASI Series Vol. **H46**, 63–85

Terry, B.R., Robards, A.W. (1987) Hydrodynamic radius alone governs the mobility of molecules through plasmodesmata. Planta **171**, 145–157

Tucker, E.B. (1982) Translocation in the staminal hairs of *Setcreasea purpurea*. I A study of ultrastructure and cell-to-cell passage of molecular probes. Protoplasma **113**, 193–201

Tucker, E.B. (1988) Inositol bisphosphate and inositol trisphosphate inhibit cell-to-cell passage of carboxyfluorescein in staminal hairs of *Setcreasea purpurea*. Planta **174**, 358–363

Tucker, E.B. (1990) Calcium-loaded 1,2-bis(2-aminophenoxy) ethane-N,N,N,N′ -tetraacetic acid blocks cell-to-cell diffusion of carboxyfluorescein in staminal hairs of *Setcreasea purpurea*. Planta **182**, 34–38

Turin, L. (1984) The basics of electrical coupling. NATO ASI Series Vol. **A99**, 285–296

Vorob'ev, L.N., Tarkhanov, K.A., Vakhmistrov, D.B. (1982) Use of electrical coupling factor for quantitative estimation of symplastic communications. Soviet Plant Physiol. **28**, 495–502

Williamson, R.E. (1992) Cytoplasmic streaming in Characean algae: mechanism, regulation by Ca^{2+}, and organization. In: Algal cell motility, pp. 73–98, Melkonian, M., ed. Chapman and Hall, New York London